nature COMMUNICATIONS

ARTICLE

Received 27 Apr 2015 | Accepted 14 Jul 2015 | Published 20 Aug 2015

DOI: 10.1038/ncomms9060

Integration of carbohydrate metabolism and redox state controls dauer larva formation in *Caenorhabditis elegans*

Sider Penkov[1], Damla Kaptan[1], Cihan Erkut[1], Mihail Sarov[1], Fanny Mende[1] & Teymuras V. Kurzchalia[1]

Under adverse conditions, *Caenorhabditis elegans* enters a diapause stage called the dauer larva. External cues signal the nuclear hormone receptor DAF-12, the activity of which is regulated by its ligands: dafachronic acids (DAs). DAs are synthesized from cholesterol, with the last synthesis step requiring NADPH, and their absence stimulates dauer formation. Here we show that NADPH levels determine dauer formation in a regulatory mechanism involving key carbohydrate and redox metabolic enzymes. Elevated trehalose biosynthesis diverts glucose-6-phosphate from the pentose phosphate pathway, which is the major source of cellular NADPH. This enhances dauer formation due to the decrease in the DA level. Moreover, DAF-12, in cooperation with DAF-16/FoxO, induces negative feedback of DA synthesis via activation of the trehalose-producing enzymes TPS-1/2 and inhibition of the NADPH-producing enzyme IDH-1. Thus, the dauer developmental decision is controlled by integration of the metabolic flux of carbohydrates and cellular redox potential.

[1] Max Planck Institute of Molecular Cell Biology and Genetics, Dresden 01307, Germany. Correspondence and requests for materials should be addressed to T.V.K. (email: kurzchalia@mpi-cbg.de).

When overcrowded or starved, *Caenorhabditis elegans* interrupts its reproductive cycle to enter diapause by forming a dauer (enduring) larva[1]. Dauer larvae can withstand extreme conditions such as treatment with strong detergents and severe desiccation[2,3]. This increased stress resistance is due to the reprogramming of gene expression that is radically different from that of reproductive larvae[4,5]. Similar gene expression changes are also found in long-living mutants[6]. Dauer larvae are broadly used as a paradigm for studying hypometabolism and metabolism during starvation[7]. Thus, understanding the mechanisms of dauer formation can shed light on general processes, such as ageing and decreased metabolic activity.

Biochemical and genetic studies show that dauer formation is initiated by specific short-chain ascarosides acting as dauer-inducing pheromones[8,9] and is controlled by the so-called *daf* genes (for abnormal *da*uer *f*ormation). Three signalling pathways, namely the transforming growth factor (TGF)-β-like (defined by the TGF-β homologue DAF-7), insulin-like (defined by the insulin receptor homologue DAF-2) and cyclic GMP pathways[1], converge on the activity of a nuclear hormone receptor/transcription factor, DAF-12 (refs 10,11). DAF-12 binds sterol-derived, bile acid-like molecules known as dafachronic acids (DAs)[12,13]. The last, crucial reaction in DA biosynthesis is catalysed by cytochrome P450 (CYP450) DAF-9, which produces a carboxyl group at the C-26 methyl residue of the precursor in three oxidation steps. This reaction requires NADPH[13]. DAF-9 is expressed in a pair of DA-secreting neuroendocrine cells called the XXX cells[14]. DAF-9 expression is also observed in the hypodermis, which is the syncytial epidermal tissue that surrounds the worm[14]. Secreted DAs act to suppress dauer-promoting activity of DAF-12 at the organism-wide level, and worms remain in the reproductive cycle[13].

Downregulation of DAF-7 or DAF-2 presumably reduces the level of available DA by inhibiting its synthesis, degrading it or sequestering it in an inactive form. One of the mechanisms regulating biosynthesis of DA may be the modulation of the concentration of substrates required for its synthesis. Recently, we showed that methylation of cholesterol in the fourth position by the sterol methylase STRM-1 renders cholesterol unsuitable for DA synthesis[15]. Another cofactor for DA production is cytosolic NADPH, which is used by DAF-9 as an electron donor[13]. Before this study, no information regarding the involvement of NADPH in the regulation of DA synthesis was available.

Here we show that the level of cytosolic NADPH determines dauer formation and is regulated by the biosynthesis of the disaccharide trehalose, which diverts glucose-6-phosphate (G6P) from the pentose phosphate pathway (PPP), the major source of NADPH in the cell. We also show that DAF-12 negatively regulates DA production by two parallel mechanisms. First, DAF-12 increases the biosynthesis of trehalose by activating the enzymes TPS-1 and TPS-2. Second, DAF-12 downregulates IDH-1, another enzyme involved in NADPH production in the cytosol. Thus, the developmental switch (reproductive to dauer) is directly connected to the metabolic flux of carbohydrates as well as to cellular redox potential.

Results

Trehalose-deficient mutants exhibit reduced dauer formation. Recently, we showed that dauer larvae produce stage-specific glycolipids (maradolipids) containing the disaccharide trehalose[16]. Here we exploited a *C. elegans* strain that was unable to synthesize trehalose to investigate whether trehalose production could also be involved in the determination of dauer fate.

C. elegans produces trehalose from G6P and UDP-glucose in a two-step reaction[17,18]. In the first step, trehalose-6-phosphate is synthesized by trehalose-6-phosphate synthase (TPS), which is encoded by the genes *tps-1* and *tps-2*. Next, the phosphate is removed by trehalose-6-phosphate phosphatase. We produced a mutant *C. elegans* strain that lacked functional TPS-1 and TPS-2 proteins (ΔΔ*tps*) and consequently was unable to synthesize trehalose[16].

We noticed that ΔΔ*tps* had a reduced number of dauers when grown in a liquid culture at high population density. The ΔΔ*tps* dauers, however, had proper dauer morphology as examined using electron microscopy[16] and were resistant to SDS treatment. To investigate the dauer formation in ΔΔ*tps* under controlled conditions, we tested dauer formation in the presence of synthetic dauer-inducing pheromones. As seen in Fig. 1a, ΔΔ*tps* formed approximately sevenfold fewer dauers than wild-type worms. This suggests that biosynthesis of trehalose is involved in the regulation of dauer formation.

Next, we investigated the connection between the biosynthesis of trehalose and the major dauer-regulatory pathways. The TGF-β (*daf-7*) pathway acts downstream of dauer-inducing pheromones[19,20]. A *C. elegans* strain bearing the *daf-7 (e1372)* allele has a dauer-constitutive (Daf-c) phenotype and forms ∼100% dauers at 25 °C (restrictive temperature) and ∼50% dauers at 20 °C (semipermissive temperature)[21]. To investigate whether *tps-1* and *tps-2* genetically interact with *daf-7*, we introduced ΔΔ*tps* to a *daf-7* background. As seen in Fig. 1b, the deficiency in trehalose biosynthesis significantly reduced the Daf-c phenotype of *daf-7* at the semipermissive temperature (20 °C). Moreover, ΔΔ*tps* decreased dauer formation of *daf-7* even at 25 °C when the L1 larvae were starved for 48 h before being transferred to the restrictive temperature (Fig. 1b). This effect was probably caused by the increase in DAF-9 expression on starvation, as described previously[22]. Thus, ΔΔ*tps* leads to a conditional, dauer-defective (Daf-d) phenotype and genetically interacts with the *daf-7* pathway.

In parallel to DAF-7, dauer formation is controlled by the insulin receptor-like protein DAF-2 (ref. 23). Mutation of this protein leads to a Daf-c phenotype[24]. Two distinct classes of *daf-2* Daf-c alleles exist that are classified according to the ability of *daf-12* Daf-d mutations to suppress the Daf-c phenotype and restore the reproductive development. Class I alleles (for example, *daf-2(e1368)*) are rescued; however, class II alleles (for example, *daf-2(e1370)*) are not rescued by *daf-12* mutations[24]. To test the genetic interaction of *tps-1/tps-2* with *daf-2*, ΔΔ*tps* was placed in the background of the thermosensitive Daf-c mutations *daf-2(e1368)* and *daf-2(e1370)*. In contrast to the *daf-7* pathway, ΔΔ*tps* could not suppress the Daf-c phenotypes of the class I or class II alleles of *daf-2* under any of the conditions tested, including starvation in L1 (Fig. 1c,d). This suggests that a decrease in insulin signalling can induce dauer formation even when trehalose cannot be produced.

The fact that biosynthesis of trehalose can influence dauer formation prompts the question as to whether this process acts upstream or downstream of the DA-producing enzyme DAF-9. To address this, we first investigated whether ΔΔ*tps* could suppress the Daf-c phenotype of *daf-9*. Mutants bearing the null allele *daf-9(dh6)* produce dauer-like larvae because DA is not synthesized[13,14,22]. In the absence of exogenous DA, the triple mutant *daf-9*;ΔΔ*tps* could not produce reproductive adults under any of the conditions tested (with or without starvation; Fig. 1e). Second, ΔΔ*tps* could not suppress the induction of wild-type dauers on substitution of cholesterol by lophenol. As previously shown, DA cannot be produced when lophenol is the only dietary sterol because cholesterol, the precursor for DA synthesis, is absent[25]. ΔΔ*tps* formed dauer larvae on lophenol and this process

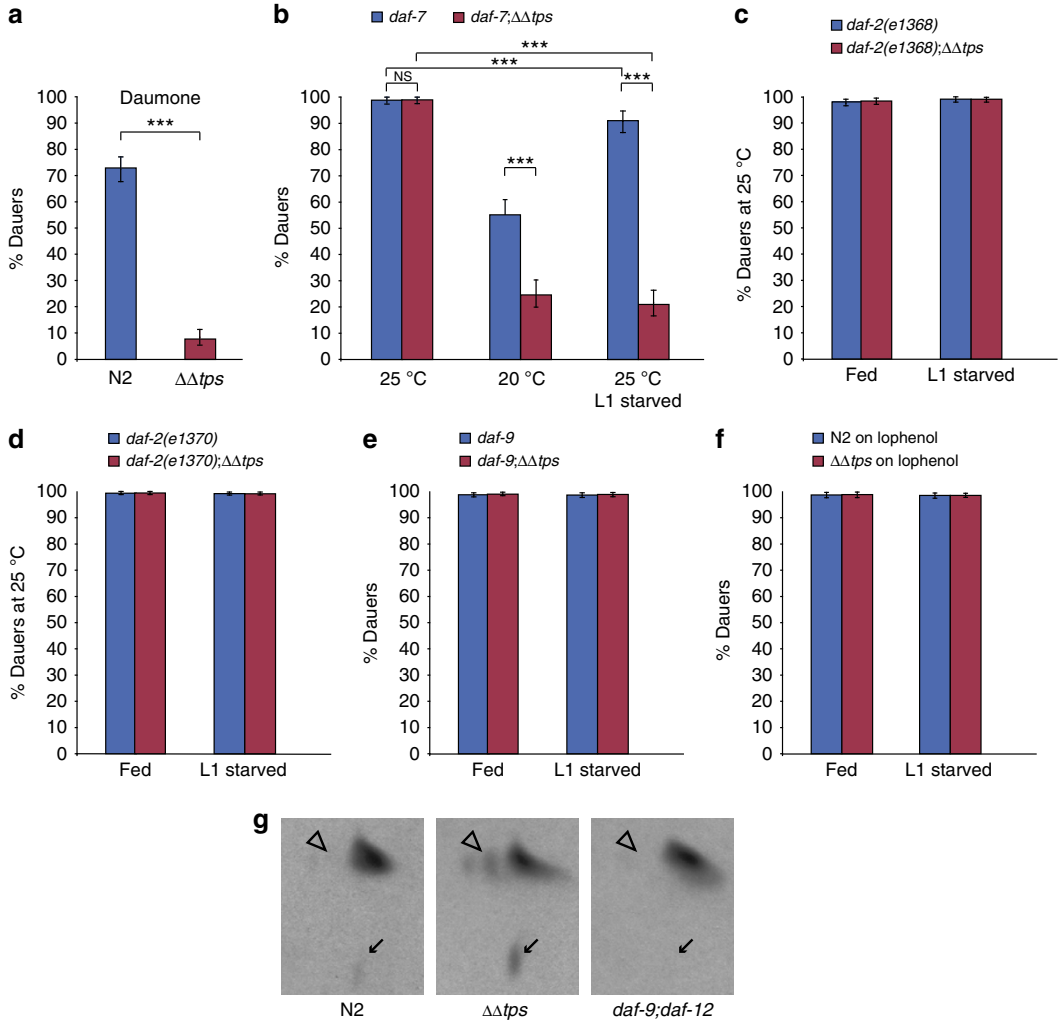

Figure 1 | Loss of TPS activity suppresses dauer formation by elevation of DA levels. (**a**) Δ*Δtps* ($n=1,070$) has diminished sensitivity to dauer pheromones in comparison with the wild type (N2, $n=1,277$). (**b**) Dauer formation of *daf-7* and *daf-7;*Δ*Δtps*. Δ*Δtps* causes a decrease in the Daf-c phenotype of *daf-7* at the semipermissive temperature (20 °C) and, when starved in L1 larva, at the restrictive temperature (25 °C). For *daf-7*: 25 °C $n=808$, 20 °C $n=755$, 25 °C L1 starved $n=855$. For *daf-7;*Δ*Δtps*: 25 °C $n=906$, 20 °C $n=744$, 25 °C L1 starved $n=697$. (**c**) Dauer formation of *daf-2(e1368)* and *daf-2(e1368);*Δ*Δtps* at restrictive temperature with or without starvation in L1. Δ*Δtps* does not change the dauer formation of *daf-2(e1368)*. For *daf-2(e1368)*: fed $n=627$, L1 starved $n=566$. For *daf-2(e1368);*Δ*Δtps*: fed $n=705$, L1 starved $n=650$. (**d**) Dauer formation of *daf-2(e1370)* and *daf-2(e1370);*Δ*Δtps* at restrictive temperature. Starvation in L1 was also examined. Δ*Δtps* does not change the dauer formation of *daf-2(e1370)*. For *daf-2(e1370)*: fed $n=618$, L1 starved $n=660$. For *daf-2(e1370);*Δ*Δtps*: fed $n=452$, L1 starved $n=446$. (**e**) Dauer formation of *daf-9* and *daf-9;*Δ*Δtps* with or without starvation in L1. Δ*Δtps* does not change the formation of dauer larvae of *daf-9*. For *daf-9*: fed $n=231$, L1 starved $n=231$. For *daf-9;*Δ*Δtps*: fed $n=204$, L1 starved $n=220$. (**f**) Dauer formation observed on medium in which cholesterol is replaced by lophenol with or without starvation in L1. Δ*Δtps* is not sufficient for a substantial decrease in dauer larvae. For N2: fed $n=512$, L1 starved $n=533$. For Δ*Δtps*: fed $n=445$, L1 starved $n=412$. (**g**) Detection of DA (arrowheads) and the putative (25*S*)-3α-hydroxy-7-cholestanoic acid (arrows) by 2D-TLC of extracts of ^{3}H-cholesterol labelled worms. Δ*Δtps* has increased intensity of the DA and cholestanoic acid bands in comparison with the wild-type (N2). *daf-9;daf-12* is unable to produce DA and cholestanoic acid because it lacks DAF-9. Scans of whole TLC plates are shown in Supplementary Fig. 1. In (**a**–**f**), data were collected from at least four biological replicates, from at least two experiments. In **g**, representative images from two experiments. Error bars represent 95% confidence intervals. Means, confidence intervals and statistical significance were modelled by beta regression analysis. ***$P<0.001$; ns, no significant difference (beta regression).

was not decreased by starvation (Fig. 1f). Since the absence of trehalose does not suppress either the null mutant of *daf-9* or the absence of substrate for DA synthesis, it can be surmised that trehalose acts upstream or at the level of DAF-9.

In the light of these findings, we expected that the absence of trehalose synthesis would increase the amount of DA. This hypothesis was tested by labelling worms with radioactive cholesterol and analysing the lipid extracts by two-dimensional (2D) thin-layer chromatography (2D-TLC). As seen in Fig. 1g and Supplementary Fig. 1, Δ*Δtps* produced substantially more DA than the wild type. A compound probably corresponding to (25*S*)-3α-hydroxy-7-cholestanoic acid, a reduced form of DA that has also been proposed as an endogenous ligand of DAF-12 (refs 12,15,26) was also elevated in Δ*Δtps* (Fig. 1g).

Overexpression of TPS-1 enhances dauer formation. Deficiency of trehalose biosynthesis resulted in decreased dauer formation. We therefore reasoned that overproduction of trehalose might have the opposite effect. A transgenic approach was employed to overexpress TPS[27]. We chose to overexpress one of the TPS enzymes, TPS-1. TPS-1 and TPS-2 have largely overlapping

expression patterns and share high sequence similarity (54% identity, 71% similarity, WormBase WS246). A worm expression vector was constructed that contained eGFP (enhanced green fluorescent protein)-tagged *tps-1* downstream of the putative endogenous *tps-1* promoter (Fig. 2a). Transformed worm strains bearing an extrachromosomal array were selected as these presumably held multiple copies of the construct.

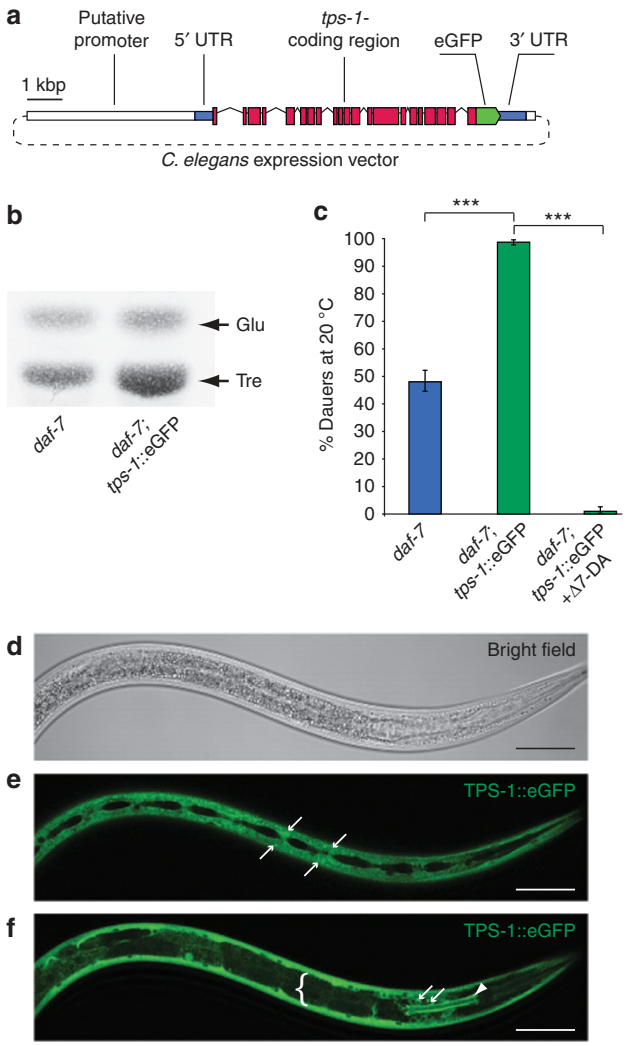

Figure 2 | Overexpression of TPS-1 leads to elevation of trehalose levels and dauer formation. (**a**) Design of the modified fosmid construct used for overexpression of TPS-1 in *daf-7*. The construct contains the *tps-1*-coding sequence tagged with eGFP at the C terminus with the corresponding endogenous 5′-untranslated region (UTR), 3′-UTR and ~5 kb promoter region. (**b**) TLC of sugars from *daf-7* and *daf-7;tps-1*::eGFP. Sugars were visualized with Molisch reagent (Tre—trehalose R_f ~0.46, Glu—glucose R_f ~0.57). A scan of the whole TLC plate is shown in Supplementary Fig. 2. (**c**) Dauer formation of *daf-7* and *daf-7;tps-1*::eGFP at 20 °C. Overexpression of TPS-1 enhances the Daf-c phenotype of *daf-7*, but the dauer formation is abolished in DA-fed animals. *daf-7* $n = 746$, *daf-7;tps-1*::eGFP $n = 756$, *daf-7; tps-1*::eGFP + DA $n = 660$. (**d**) Transmitted light micrograph of a *daf-7; tps-1*::eGFP animal grown at 20 °C. (**e**) Confocal scanning micrograph of the animal in **d**. TPS-1::eGFP fluorescence is detected in hypodermal syncytium (arrows). (**f**) In addition, TPS-1::eGFP is located to the isthmus of the pharynx (arrowhead) and the cell bodies of various head neurons (arrows). Intestinal cells are completely devoid of TPS-1::eGFP signal (curly bracket). Scale bars in **d**–**f**, 20 µm. In **b**,**d**,**e**,**f**, representative images from at least two experiments. In **c**, data were collected from six biological replicates from three independent experiments. Error bars represent 95% confidence intervals. Means, confidence intervals and statistical significance were modelled by beta regression analysis. ***$P < 0.001$ (beta regression).

Under normal growth conditions, the overexpression of *tps-1* did not produce a Daf-c phenotype. To test dauer formation under mild dauer-inducing conditions, the *tps-1*-overexpressing strain was crossed to *daf-7* to obtain *daf-7;tps-1::eGFP*. Biochemical analysis showed that *daf-7;tps-1::eGFP* produced more trehalose than *daf-7* (Fig. 2b and Supplementary Fig. 2). This transgenic line was strongly Daf-c: at 20 °C, ~100% dauers were formed (Fig. 2c). The effect of *tps-1::eGFP* on dauer formation was, however, fully abolished when DA was added to the medium, again demonstrating that biosynthesis of trehalose stimulated dauer formation by interfering with DA synthesis (Fig. 2c).

Light microscopy was performed on *daf-7;tps-1*::eGFP undergoing dauer formation to investigate the localization of TPS-1 (Fig. 2d–f). Strong expression occurred predominantly in the hypodermis (Fig. 2e), a tissue in which DAF-9 and STRM-1 are also expressed[14,15,22]. Some expression was observed in a number of head neurons and in the isthmus of the pharynx, and no expression was seen in the intestinal cells (Fig. 2f). Thus, overexpression of TPS-1 might enhance dauer formation by acting in the cells responsible for DA synthesis (hypodermis).

Availability of cytosolic NADPH determines dauer formation. We next wished to investigate how the absence of trehalose might lead to a reduction in dauer formation. One possible explanation is that trehalose is itself a dauer-inducing molecule. However, feeding *daf-7* with even very high amounts of trehalose had no effect on dauer formation (Fig. 3a). Therefore, we hypothesized that the biosynthesis of trehalose and DA is coupled.

As mentioned above, trehalose is synthesized from G6P and UDP-glucose. G6P is an important molecule that stands on the crossroads of several carbohydrate pathways. One such pathway is the PPP. NADPH, a major cellular reducing agent, is essential for a wide array of anabolic processes. NADPH in the cytosol is predominantly produced from G6P in the oxidative phase of the PPP[28]. Thus, trehalose and NADPH biosyntheses are coupled by their common substrate. The electron donor in oxygenation reactions catalysed by microsomal Cyp450 systems is almost exclusively NADPH[29]. DAF-9, as a member of the Cyp450 family, is expected to also use NADPH during DA biosynthesis. Indeed, *in vitro* reactions with microsomes containing DAF-9 demonstrated a requirement for NADPH[13]. We hypothesized that increased trehalose biosynthesis would reduce the cellular NADPH level by reducing G6P consumption through the PPP. In turn, this would be expected to decrease the DA level and increase dauer formation. Accordingly, reduced TPS activity would be expected to increase the NADPH level by increasing the amount of G6P.

To determine the effect of *tps-1*/*tps-2* on the NADPH level, we designed an extraction procedure to recover nucleotides from worms. Using a 2D-TLC ion-exchange system to visualize NADPH in the nucleotide pool, we compared the NADPH levels in reproductive and dauer larvae. To produce large amounts of worms for biochemical analysis, we made use of the temperature-sensitive Daf-c mutant *daf-2(e1370)*. This mutant produces ~100% L3 larvae at 15 °C and ~100% dauer larvae at 25 °C. Generally, the NADPH levels in both L3 and dauer larvae are very low compared with those of other nucleotides such as ATP/ADP and GTP/GDP (Fig. 3b and Supplementary Fig. 3). This makes NADPH a suitable target for the regulation of Cyp450 activity. Reproductive L3 larvae showed higher levels of NADPH than those of dauer larvae (Fig. 3b and Supplementary Fig. 3).

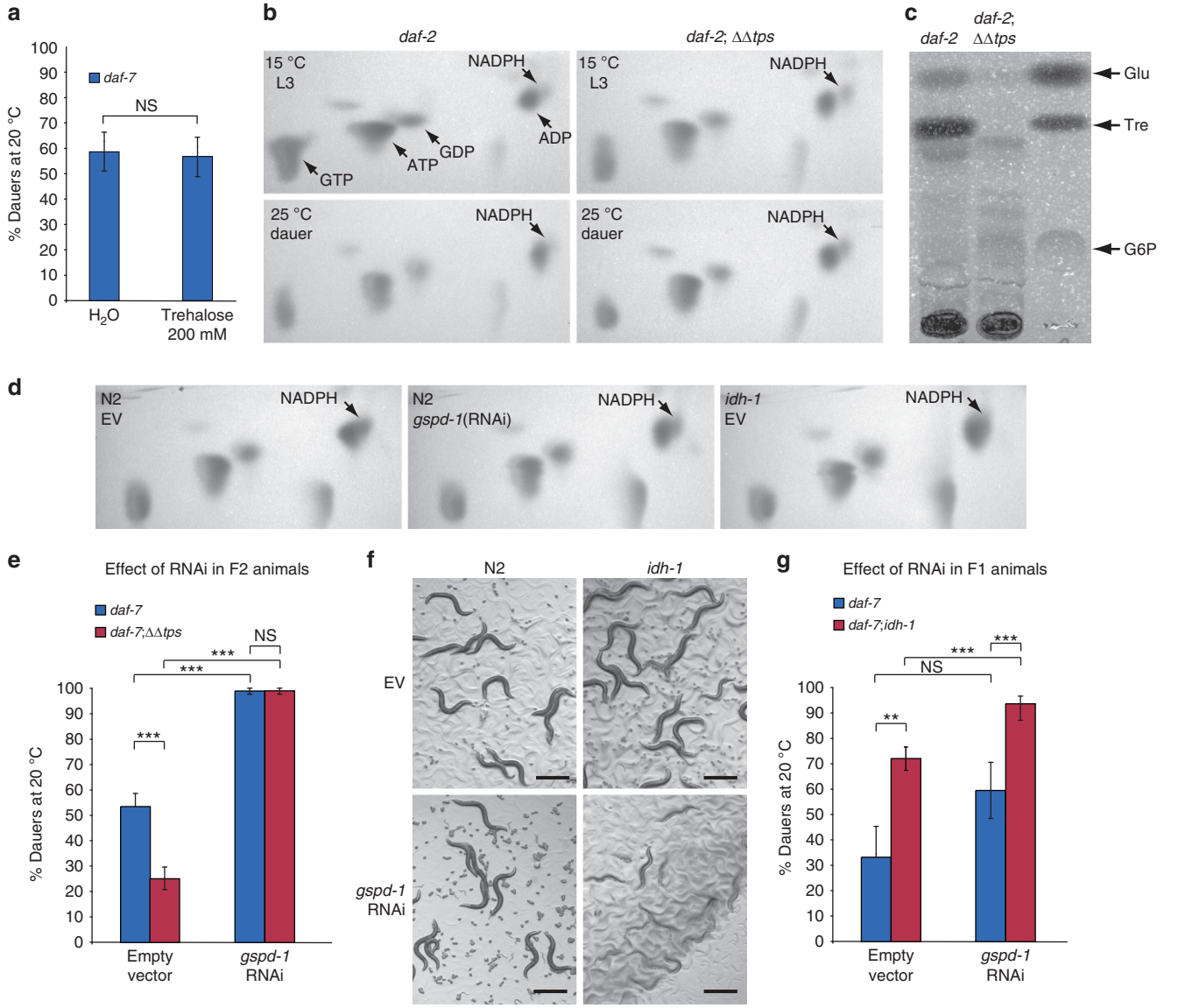

Figure 3 | Cellular NADPH levels determine dauer formation. (**a**) High concentration of trehalose in the feeding medium does not enhance the Daf-c phenotype of *daf-7*. Control (water) $n=684$, trehalose treated $n=612$. (**b**) 2D-TLC of nucleotides from *daf-2(e1370)* and *daf-2(e1370);ΔΔtps* L3 and dauer larvae. *ΔΔtps* causes marked increase in NADPH in both L3 and dauer larvae of *daf-2*. (**c**) TLC of sugars from *daf-2(e1370)* and *daf-2(e1370);ΔΔtps* dauers. Note the disappearance of the trehalose band and the accumulation of G6P in *daf-2;ΔΔtps* (G6P—glucose-6-phosphate $R_f \sim 0.17$, Tre—trehalose $R_f \sim 0.46$, Glu—glucose $R_f \sim 0.57$). (**d**) 2D-TLC of nucleotides derived from wild-type (N2) L3 larvae after two generations on empty vector control RNAi (EV) or *gspd-1*(RNAi) and *idh-1(ok2832)* on EV. Note the reduction of the NADPH levels caused by *gspd-1*(RNAi). The mutant of *idh-1* also displays lower NADPH amounts compared with the wild type. Scans of whole TLC plates are shown in Supplementary Figs 3–5. (**e**) Dauer formation of *daf-7* and *daf-7;ΔΔtps* on *gspd-1*(RNAi) at 20 °C. *gspd-1* (RNAi) leads to an increase in the incidence of dauers. For *daf-7*: EV $n=775$, *gspd-1* (RNAi) $n=782$. For *daf-7;ΔΔtps*: empty vector $n=814$, *gspd-1* (RNAi) $n=734$. (**f**) When PPP is partially inactivated by RNAi against *gspd-1*, in the first generation the wild-type worms do not have obvious defects. Under the same conditions, *idh-1* mutants display pronounced slow growth, sick and reduced body size phenotypes. Scale bars, 500 μm. (**g**) Dauer formation of *daf-7* and *daf-7;idh-1* on *gspd-1* (RNAi) at 20 °C. *daf-7;idh-1* shows higher incidence of dauers compared with *daf-7* and it is further enhanced by *gspd-1* (RNAi). For *daf-7*: empty vector $n=823$, *gspd-1* (RNAi) $n=858$. For *daf-7;idh-1*: EV $n=1098$, *gspd-1* (RNAi) $n=834$. In **b**,**c**,**d**,**f**, representative images from at least two experiments. In **a**,**e**,**g**, data were collected from at least five biological replicates, from at least three independent experiments. Error bars represent 95% confidence intervals. Means, confidence intervals and statistical significance were modelled by beta regression analysis. ***$P<0.001$, **$P<0.01$, ns no significant difference (beta regression).

According to our hypothesis, TPS-1/2-deficient worms should produce more NADPH than worms with intact TPS enzymes. Indeed, both L3 and dauer larvae of the *daf-2;ΔΔtps* mutant exhibited higher NADPH levels than those of corresponding stages of the *daf-2* mutant (Fig. 3b and Supplementary Fig. 3). Moreover, the G6P level was higher in the dauer larvae of *daf-2;ΔΔtps* than in those of *daf-2* (Fig. 3c and Supplementary Fig. 4).

Next, we tested whether the depletion of cytosolic NADPH enhances dauer formation. The first and rate-limiting enzyme of the PPP, G6P dehydrogenase, produces NADPH and phosphogluconolactone from G6P in the cytosol[28]. Inactivation of this enzyme disrupts the entire oxidative phase of the PPP and leads to grave pathologies, such as haemolytic anaemia, due to a decreased redox potential[28]. This enzyme is encoded by a single gene in *C. elegans*, *gspd-1*. Loss-of-function mutations of *gspd-1*

are lethal; therefore, we decided to use an RNA interference (RNAi) approach. RNAi against *gspd-1* had a strong pleiotropic phenotype of slow growth and a sick appearance, but not of constitutive dauer formation, in reproducing wild-type worms of the second generation[30]. The worms also displayed markedly lower NADPH levels (Fig. 3d and Supplementary Fig. 5). Remarkably, two generations of RNAi of *gspd-1* in the *daf-7* or *daf-7;ΔΔtps* backgrounds led to ~100% dauer formation at 20 °C (Fig. 3e).

Apart from the oxidative phase of the PPP, the second source of cytosolic NADPH in cells is oxidative decarboxylation of isocitrate to 2-oxoglutarate by the enzyme isocitrate dehydrogenase 1 (cytosolic)[31]. In *C. elegans*, this enzyme is encoded by the gene *idh-1*. The mutant *idh-1(ok2832)*, which bears a large insertion/deletion that eliminates a substantial part of the *idh-1*-coding region, is viable, presumably because the PPP continues to furnish a sufficient level of cytosolic NADPH (Fig. 3d and Supplementary Fig. 5). Indeed, when RNAi against *gspd-1* was applied to *idh-1*, it resulted in a strong growth delay, a sick appearance and a small body size as early as the first generation (Fig. 3f). This treatment, however, did not result in a Daf-c phenotype. To test the influence of *idh-1* on dauer formation, we produced a *daf-7(e1372);idh-1(ok2832)* double mutant. At 20 °C, *daf-7;idh-1* produced ~26% more dauers than *daf-7* (Fig. 3g). When PPP was inhibited by *gspd-1* (RNAi), the formation of dauers in *daf-7;idh-1* in the first generation was increased to >90% (Fig. 3g). Therefore, the level of cytosolic NADPH directly regulates dauer formation.

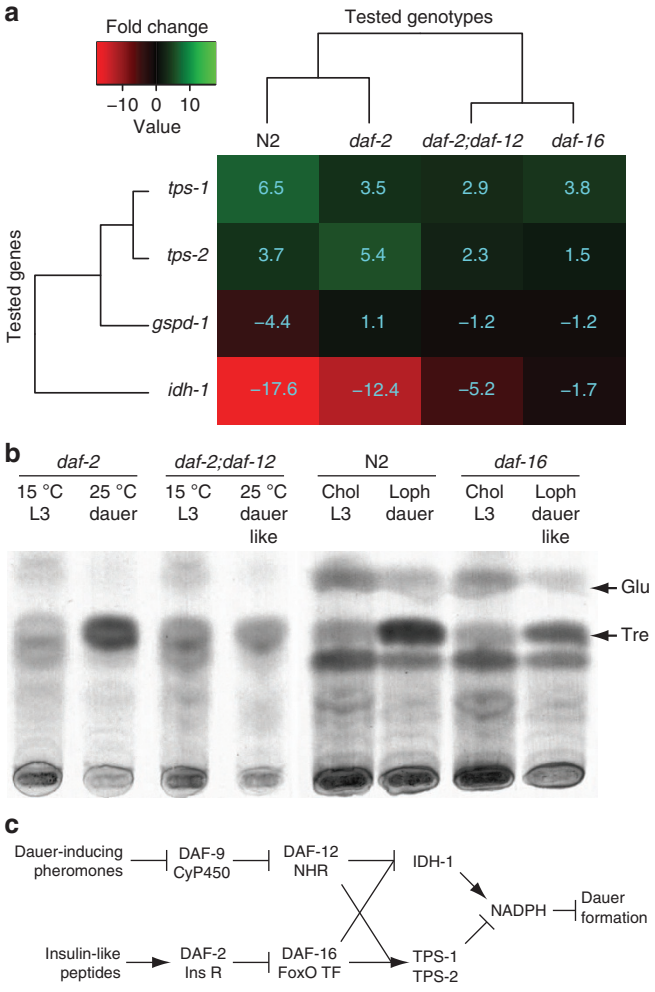

Figure 4 | DAF-12 and DAF-16 regulate the synthesis of trehalose and NADPH. (**a**) Heat map of the differential expression of *gspd-1*, *tps-1*, *tps-2* and *idh-1* genes in *daf-2*, *daf-2;daf-12*, N2 wild-type and *daf-16* worms measured using qRT–PCR. The heat map represents the fold change of the expression of the genes in dauer(-like) larvae compared with L3 larvae. (**b**) TLC of ^{14}C-acetic acid-labelled sugars and lipids from *daf-2* and *daf-2;daf-12* at 15 or 25 °C and from N2 and *daf-16* grown on cholesterol or on lophenol (Tre—trehalose R_f ~0.35; Glu—glucose R_f ~0.5). Scans of whole TLC plates are shown in Supplementary Fig. 6. (**c**) Dauer formation is controlled by DAF-12 and DAF-16 in a mechanism that involves the production of NADPH. Activation of DAF-12 in response to dauer-inducing pheromones and activation of DAF-16 in response to reduced insulin signalling are both necessary for the activation of TPS-1/2 and the inhibition of IDH-1. As a result, the synthesis of NADPH is diminished and this leads to decrease in DAs and ultimately to dauer formation. In **a**, expression levels were measured in three biological replicates. In **b**, representative images from two experiments.

DAF-16 and DAF-12 regulate cytosolic NADPH levels. As shown above, the biosynthesis of trehalose influences the dauer developmental transition by interfering with the synthesis of NADPH and DA. However, it remained unclear how this process is used in *C. elegans* as a mechanism to regulate dauer formation. We considered DAF-16 to be one of the possible candidates for regulating this process. It was previously demonstrated that the inhibition of insulin signalling and subsequent activation of DAF-16 leads to the upregulation of *tps-1* and *tps-2* in the determination of adult longevity and adaptation to hyperosmotic conditions[32,33]. In dauer formation, however, one of the main functions of DAF-16 is to regulate the activity of DAF-9 and, consequently, DAF-12 (ref. 34). Thus, during dauer formation, DAF-16 might induce the expression of *tps-1*/*tps-2* via activation of DAF-12 or via an independent mechanism. Conversely, we recently showed that DAF-12 regulates dauer formation via a negative feedback loop by decreasing one of the substrates used for DA synthesis, cholesterol. DAF-12 activates STRM-1, a methylase that renders cholesterol unsuitable for DA synthesis[15]. Thus, DAF-16 and/or DAF-12 could act in a similar way to decrease the level of NADPH, the other substrate for DA synthesis, for example, by activation of TPS-1/2 or downregulation of the activity of PPP and/or IDH-1.

We tested the contributions of DAF-16 and DAF-12 to cytosolic NADPH levels using conditions/strains in which either DAF-16 was active but DAF-12 was not, or DAF-12 was active but DAF-16 was not. As mentioned above, class II alleles of *daf-2* are not suppressed by *daf-12* Daf-d mutations and *daf-2;daf-12* double mutants typically arrest as dauer-like larvae due to the activation of DAF-16 (ref. 24). Conversely, activation of DAF-12 caused by mutation of *daf-9* or substitution of the dietary cholesterol with lophenol also induces the formation of arrested dauer-like larvae in *daf-16* loss-of-function mutants[25,35].

First, we used qRT–PCR to examine the expression of *tps-1* and *tps-2* in *daf-2(e1370)* and *daf-2(e1370);daf-12(rh61rh411)* worms. Worms were grown at 25 °C to induce arrest as dauer (*daf-2*) or dauer-like (*daf-2;daf-12*) larvae. Expression of *tps-1* and *tps-2* in these worms was compared with that in L3 larvae of the same strains grown at 15 °C. Pronounced upregulation of *tps-1* and *tps-2* was observed in *daf-2* dauers (Fig. 4a). In *daf-2;daf-12* dauer-like animals, *tps-1* and *tps-2* were also upregulated, but to a lesser degree than in *daf-2* (Fig. 4a). Next, we compared the expression of *tps-1* and *tps-2* in lophenol-induced wild-type (N2) and *daf-16(mu86)* dauer(-like) larvae with that in cholesterol-grown L3 larvae of the same strains. Both *tps* genes were upregulated in the dauer(-like) stage, but the upregulation was less pronounced in *daf-16* dauer-like larvae than in N2 dauers

(Fig. 4a). This demonstrates that DAF-16 and DAF-12 are both sufficient to activate the transcription of *tps-1* and *tps-2*, but that expression of the *tps* genes is roughly doubled if both DAF-16 and DAF-12 are active.

To test whether the decrease in *tps-1/2* transcriptional activity in *daf-2;daf-12* and *daf-16* dauer-like larvae results in decreased synthesis of trehalose, we performed TLC of sugars derived from ^{14}C-acetate-labelled animals. First, we compared *daf-2* and *daf-2;daf-12*. L3 larvae of both strains contained a basal amount of trehalose, which was higher in *daf-2* dauers but unchanged in *daf-2;daf-12* dauer-like animals (Fig. 4b and Supplementary Fig. 6). Similarly, ^{14}C-acetate-labelled N2 lophenol dauers had much higher trehalose levels than those of cholesterol-fed L3 larvae of the same strain. By contrast, the trehalose level in *daf-16* lophenol dauer-like larvae was only slightly higher than that in *daf-16* L3 larvae (Fig. 4b and Supplementary Fig. 6). Thus, DAF-12 and DAF-16 are both necessary for the increase in trehalose biosynthesis and presumably act at the transcriptional level to modulate the enzymatic activity of TPS-1/2.

The abundance of NADPH in the cytosol could also be diminished by downregulation of the activity of PPP NADPH-producing enzymes. However, as shown in Fig. 4a, the expression of *gspd-1* in *daf-2* and *daf-2;daf-12* dauer (-like) larvae is not substantially different from that in L3 larvae. Compared with L3 larvae, *gspd-1* (~4.4-fold) expression was lower in N2 lophenol dauers; however, almost no change was observed in *daf-16* lophenol dauer-like larvae (Fig. 4a). Thus, this enzyme does not seem to be regulated at the transcriptional level.

As an alternative source of cytosolic NADPH, IDH-1 activity could also be controlled by DAF-16 and/or DAF-12. Indeed, quantitative reverse transcription–PCR (qRT–PCR) analysis showed that *idh-1* expression was lower in both *daf-2* and *daf-2;daf-12* worms at 25 °C than in the same worms at 15 °C (Fig. 4a). However, this decrease was much more pronounced in *daf-2* (~12.4-fold) than in *daf-2;daf-12* (~5.2-fold). Similarly, N2 lophenol-induced dauers showed a much lower expression level of *idh-1* than cholesterol-fed L3 larvae (~17.6-fold), whereas *idh-1* expression in *daf-16* lophenol-grown dauer-like animals was only ~1.7-fold lower than in *daf-16* cholesterol-fed L3 larvae (Fig. 4a). These results indicate that DAF-12 and DAF-16 are both necessary for strong downregulation of IDH-1. This finding also suggests that IDH-1, together with TPS-1/2, is a major target of DAF-16 and DAF-12 in the control of cytosolic NADPH levels.

Discussion

This study investigated how carbohydrate metabolism and NADPH availability affect dauer formation. The dauer formation process involves the biosynthesis of trehalose: in mutants unable to synthesize trehalose, dauer formation is strongly reduced. However, our study shows that it is not the presence or absence of trehalose itself that is important for dauer formation, but its biosynthesis. On the basis of our data, we suggest a mechanism to explain how this metabolic pathway regulates dauer formation. TPS-1 and TPS-2 consume G6P in hypodermal cells where DAF-9 is active. G6P is at the crossroads of several carbohydrate pathways, namely, glycolysis, gluconeogenesis, PPP and glycogen and trehalose biosynthesis (Supplementary Fig. 7). G6P is the substrate of the first enzyme of the PPP and is a major source of cytosolic NADPH, a cofactor for DA production. Thus, activation of TPS-1 and TPS-2 results in a decrease in DA synthesis and an increase in dauer formation.

Several lines of evidence support the proposed mechanism. First, the use of G6P for trehalose synthesis in worms affects NADPH levels, and these levels correlate with the formation of dauers or entry into the reproductive pathway. Inhibition of GSPD-1 and IDH-1, which are the major enzymes needed for NADPH production in the cytosol, strongly enhances dauer arrest. In addition, RNAi against *gspd-1* abolished the effect of the absence of trehalose biosynthesis. Second, the expression patterns of DAF-9 and TPS-1 were very similar. As they are localized to the same cells, regulation via depletion of either substrate or cofactor can be executed within the cell. This is reminiscent of another dauer regulator, STRM-1, which is localized to the hypodermis where methylation of cholesterol occurs[15]. Finally, DAF-16 and DAF-12 inhibited NADPH formation at the transcriptional level by (a) enhancing trehalose biosynthetic enzymes and (b) downregulating IDH-1. In this way, DAF-12, aided by DAF-16, acts in a negative feedback loop that inhibits DA synthesis by decreasing the production of its own ligand.

We present the following model based on our observations (Fig. 4c and Supplementary Fig. 7). Dauer-inducing pheromones, through various signalling pathways, act to reduce the activity of DAF-9 (refs 19,20,34). This initial inhibition activates DAF-12, which in turn activates STRM-1 and TPS-1/TPS-2, and inhibits IDH-1. This leads to a decrease in DA caused by the depletion of substrates required for DA production, that is, cholesterol and NADPH. As a result, initial activation of DAF-12 by dauer-inducing pheromones can be enhanced many fold. To be functional, this feedback mechanism requires input from the insulin branch of the dauer-regulatory pathway. The various insulin-like peptides secreted downstream of, but also in parallel to, pheromone-activated pathways converge to regulate the activity of DAF-2 and, consequently, that of DAF-16. The activation of DAF-16 resulting from reduced insulin signalling is necessary for DAF-12-mediated activation of TPS-1/2 and inhibition of IDH-1.

Our findings suggest that G6P/NADPH availability regulates the formation of dauers under moderate dauer-inducing conditions. Δ*Δtps* does not suppress the Daf-c phenotype of *daf-7* at the restrictive temperature, unless the worms are starved in the L1 stage. This observation correlates with the well-known differential regulation of DAF-9 in the hypodermis in response to differences in the strengths of dauer-inducing stimuli[14,22,36–38]. Under conditions that favour reproductive growth, the XXX cells are the main sources of DAs and DAF-9 is only transiently expressed in the hypodermis. Under such conditions, the liganded DAF-12 activates the expression of genes required for reproductive development, while DAF-16 remains inactive. Trehalose production under such conditions is low and the expression of IDH-1 is high, providing a bigger pool of NADPH for different anabolic processes. However, under moderately dauer-inducing conditions (such as an increase in population density, food shortage and Daf-c mutations at the permissive temperature), DAF-9 activity strongly increases, resulting in the production of enough DA for reproductive development. At this stage, the metabolic activity of the hypodermis determines the outcome of DA production. Enhanced gluconeogenesis and trehalose production in response to the less favourable conditions can gradually deplete the NADPH pool and limit the production of DA. Finally, under strong dauer-inducing conditions, the expression of DAF-9 in the hypodermis is largely shut down so that no DA is produced in this tissue. In this scenario, DAF-12 and DAF-16 activities maintain the low-level production of NADPH, which further limits the production of DA, thereby increasing dauer formation.

One of the major conclusions of our study is that a general biochemical pathway can be used as an indicator/executor of a developmental process. The level of G6P that marks the overall metabolic status of the cell determines the amount of a hormone (DA), which in turn determines a developmental transition

(reproductive development to dauer formation). Although DA levels are normally regulated by dauer-inducing pheromones or food signals, it now appears probable that the internal metabolic state of the organism also regulates dauer formation. Therefore, we propose a regulatory mechanism that integrates internal metabolic states with dauer signalling pathways to determine dauer developmental fate.

Our findings stress the importance of regulating general biochemical processes at the local level in cells. During dauer formation, NADPH, a major reducing agent, is required for the production of fatty acids and depository triglycerides[4,39]. A shutdown of the PPP at the organismal level would thus be deleterious for the long-term survival of the dauers. This is why DA and fatty-acid production are spatially separated in the hypodermis and gut, respectively. Lower G6P and NADPH levels in hypodermal cells, induced by the stimulation of trehalose biosynthesis, have no effect on the accumulation of fatty acids and consequently on triglyceride levels in the gut. Future studies may help reveal further interconnections between basic biochemical processes and developmental switches in worms and other organisms.

Methods

Materials. Lophenol was purchased from Research Plus (Manasquan, NJ USA), [1,2,6,7-^{3}H]-cholesterol from Biotrends (Cologne, Germany), [1-^{14}C]-acetate from HARTMANN ANALYTIC (Braunschweig, Germany), synthetic daumone from KDR Biotech Co. (South Korea) and Dulbecco's medium from Invitrogen (Karlsruhe, Germany). Short ascaroside derivative of 8*R*-hydroxy-2*E*-nonenoic acid and (25*S*)-Δ^{7}-DAs were produced at the Knölker Laboratory[40–42]. All other chemicals were purchased from Sigma-Aldrich (Taufkirchen, Germany).

The Caenorhabditis Genetics Centre provided all single mutants. All single mutants were outcrossed at least three times. Compound mutant and transgenic strains were produced during this study or past studies as published[15,16] or described below. *daf-9(dh6);dhEx24* and *daf-9(dh6);daf-12(rh61rh411)* were provided by the group of Dr A. Antebi. A list of *C. elegans* strains can be found in Supplementary Table 1.

Growth and maintenance of worm strains. Worms were routinely propagated on nematode growth medium (NGM) agar plates seeded with *E. coli* NA22 (ref. 43). Saturated cultures of *E. coli* NA22 grown in lysogeny broth (LB) medium were concentrated 10 times and spread on NGM-agar plates. Worms were placed on the plates either as mixed stage populations or as embryos obtained by hypochlorite treatment. The temperature-sensitive Daf-c mutants were grown at 15 °C to grow in the reproductive mode and at 25 °C to arrest as dauer larvae. To obtain lophenol-induced dauer and dauer-like larvae of N2 and *daf-16(mu86)*, two generations of worms were grown on sterol-depleted solid medium complemented with lophenol[25]. To produce sterol-depleted medium, the agar was replaced by agarose (Sigma-Aldrich) that was washed three times with chloroform to deplete the trace sterols in it. *E. coli* NA22 was grown in low-glucose, sterol-free DMEM culture medium (Sigma-Aldrich). Bacteria were rinsed with M9 before use. To prepare sterol-containing plates, lophenol or cholesterol 13 mM solutions in ethanol were added to bacteria and the bacteria were spread on the cholesterol-free agarose plates. The final concentration of the sterols was set to 13 μM according to the volume of the agarose plates.

Dauer formation assays. Overall, 100–150 embryos were transferred to NGM plates seeded with *E. coli* (NA22), grown at 20 or 25 °C for 3–4 days, and scored for the percentage of dauer larvae. When indicated, trehalose was added to both NGM-agar and bacteria to a final concentration of 200 mM.

To determine the effect of starvation during the L1 stage, embryos were transferred to lipid-extracted agarose plates[25] without food and starved for 48 h at 15 °C, and then transferred to NGM plates with *E. coli* at 25 °C and scored for percentage of dauers.

Dauer formation assay with synthetic dauer-inducing pheromones was performed on the basis of previous studies[9,15]. Two synthetic dauer-inducing pheromones: daumone (KDR Biotech Co.) and short ascaroside derivative of 8*R*-hydroxy-2*E*-nonenoic acid[41] were mixed both to NGM and to heat-inactivated NA22 bacteria in equal portions so that the final concentration of each compound was 20 μM. Adult worms were placed to lay eggs (~100 eggs per replicate). After 3 days at 25 °C, the plates were scored for dauer formation.

To determine dauer formation of *daf-9* and *daf-9;ΔΔtps*, ~150 bleached embryos of *daf-9;dhEx24* and *daf-9;ΔΔtps;dhEx24* were examined on NGM plates with *E. coli*. Another fraction was starved in L1, as described above, and then transferred to plates with food. *dhEx24* is an extrachromosomal array carrying active DAF-9 and nuclear GFP[14]. After 3 days *daf-9* and *daf-9;ΔΔtps* were identified on the basis of the absence of GFP signal and dauer formation was scored.

Formation of the wild type and *ΔΔtps* dauers on lophenol-containing plates was examined in the following way[25]. Two generations of worms were grown on sterol-depleted solid medium complemented with lophenol, and dauer formation was determined in the second generation. When indicated, second-generation L1 larvae were starved as described above.

In all dauer formation assays, data were collected from at least five biological replicates obtained from at least two experiments. The sample size of each biological replicate was between 45 and 300 animals to ensure power to detect changes in dauer formation. Animals were excluded from the analysis in case of premature embryonic or larval arrest. No randomization was used and the investigator was not blinded during the experiments. A generalized linear model on the basis of beta distribution and logit transformation (beta regression) was used to calculate and compare average dauer formation rates between groups[5,44]. The data were tested for meeting the assumptions of the beta distribution, an estimation of the variance was made and groups were statistically compared when the variance between them was similar. Confidence intervals were also estimated from the model and were represented by error bars.

RNAi by feeding. RNAi against *gspd-1* was performed with *E. coli* HT115 double-stranded RNA (dsRNA)-producing strain from the Ahringer dsRNA-feeding library[30] of Source BioScience (UK). The construct was sequence-verified and shown to contain a large overlap with the coding sequence of *gspd-1* (Supplementary Fig. 8). RNAi was performed in two different ways, as indicated in the text. First, for testing the RNAi in the first generation, bleached embryos were seeded to RNAi plates and the resulting worms were grown at 20 °C and scored for phenotypes. Second, for the examination of the effects of RNAi in the second generation, RNAi was induced at the L3/L4 stage of worms grown at 15 °C. Bleached embryos from the resulting adults were seeded to fresh RNAi plates, grown at 20 °C for 3–4 days and scored for phenotypes or used for biochemical analysis.

Metabolic labelling. *Cholesterol labelling.* Approximately 3,000 embryos were seeded on NGM plates containing ~10 μCi of [1,2,6,7-^{3}H]-cholesterol added to NA22 bacteria and grown for 4 days until early adulthood. At this stage, worms were snap-frozen and stored at −80 °C.

Acetic acid labelling. Approximately 20,000 synchronized L1 larvae were put on seeded plates containing 10–20 μCi of [1-^{14}C]-acetic acid and grown for 3–4 days at 15 or 25 °C until L3 reproductive larvae or dauer/arrested larvae were formed, respectively. Worms were snap-frozen and stored at −80 °C.

Lipid and sugar extraction and TLC analysis. For metabolic labelling, worms were grown as described above. For non-radioactive lipid analysis, ~20,000 synchronized L1 larvae were seeded on NGM plates with NA22 bacteria and grown at 25 °C for 3 days to form dauer larvae. Worms were lysed by freezing/thawing and extracted by using the Bligh and Dyer method[45]. After phase separation, lipids and sugars were recovered from the lower and upper phases, respectively. After drying and concentration, the non-radioactive samples were normalized for the protein content of the lysate. Radioactive cholesterol and acetic acid-labelled samples were normalized for total radioactivity. Acidic compounds in ^{3}H-cholesterol samples were enriched on QAE diethyl-(2-hydroxy-propyl)aminoethyl (QAE) Sephadex (40–125 μm beads) ion-exchange column (Sigma-Aldrich). To equilibrate the column, 0.2 g of QAE Sephadex were incubated in 10 volumes of 0.2 N HCl for 30 min, washed with water to pH 7, incubated with 10 volumes of 0.2 N NaOH for 30 min, washed again with water to pH 7 and incubated in 10 volumes of 0.1 N acetic acid. Finally, the column was washed with 10 volumes of methanol, the samples were applied, washed with 10 ml of methanol and eluted with 10 ml of 0.2 N acetic acid dissolved in methanol. Samples were dried, concentrated and applied to TLC plates.

TLC was performed on 10-cm HPTLC plates (Merck, Darmstadt, Germany). Sugars were separated using chloroform–methanol–water (4:4:1) or butanol–ethanol–water (5:3:2, two consecutive TLC runs) as the running system. 2D-TLC for the detection of DAs was conducted using chloroform–methanol (24:1) as first system and chloroform–methanol–32% ammonia (60:35:5) as the second system[15]. TLC plates were sprayed with Molisch reagent for sugar detection. TLC plates containing radioactive samples were sprayed with scintillation fluid (Lumasafe, Lumac LSC B.V., Groningen, the Netherlands) and exposed to X-ray film (Kodak Biomax MR, Sigma-Aldrich).

Extraction and TLC analysis of NADPH. Worms (~30,000 dauer or L3 larvae) were grown as described above, collected and washed in ddH_2O, and pelleted by centrifugation. The worm pellets were snap-frozen in liquid nitrogen and stored at −80 °C. To the frozen worm pellets 0.71 ml of cold methanol was added, followed by sonication in ice-cold sonication bath for 10 min. The resulting methanol homogenates were vigorously mixed and left on ice for 30 min. Methyl *tert*-butyl ether (2.135 ml) was added and the sonication followed by mixing and incubation on ice was repeated. ddH_2O (0.985 ml) was added and, after sonication and

vigorous mixing, the samples were left on ice for 1 h. The suspensions were centrifuged at 4,500 r.p.m. for 10–20 min to facilitate the phase separation. The lower (aqueous) phases were collected and concentrated via drying in a speed-vac concentrator until the volume of the samples reached 200 µl. The volume of the samples was corrected with ddH_2O according to previously measured protein content and 100 µl of them were applied to polyethylenimine (PEI)-cellulose 20 × 20 cm TLC plates (Merck). 2D-TLC was performed following a procedure modified from a previous study[46]. The first dimension was performed as a stepwise elution with 0.2 M LiCl (2 min), 1 M LiCl (6 min) and 1.6 M LiCl (to the end) without drying of the TLC plates in between. After the first dimension was completed, the wet TLC plates were immersed in 100% methanol for 20 min and dried under nitrogen flow. The second dimension was performed as a stepwise elution with sodium formate—formic acid buffers, pH 3.4 in the following order: 0.5 M buffer (30 s), 2 M buffer (2 min) and 4 M buffer (to the end). After drying the plates under nitrogen flow, the TLC plates were examined under ultraviolet source (254 nm).

Quantitative real-time PCR. The differential expression of *gspd-1*, *tps-1*, *tps-2* and *idh-1* genes was measured using qRT–PCR. *daf-2(e1370)* and *daf-2(e1370);daf-12* were grown at 15 °C or 25 °C to obtain L3 larvae or dauer/dauer-like larvae, respectively. N2 and *daf-16(mu86)* were grown on cholesterol or lophenol-containing plates to obtain L3 larvae or dauer/dauer-like larvae, respectively[25]. Total RNA was isolated using the PureLink RNA Mini Kit (Ambion) and equal amounts of all samples were reverse transcribed with SuperScript III (Invitrogen) using oligo$(dT)_{12-18}$ primers. cDNA quality was tested using standard PCR. qRT–PCR was performed on Stratagene Mx3000P (Agilent Technologies) with at least three samples in duplicates. Primer sequences are presented in Supplementary Table 2. Raw SYBR green fluorescence data were analysed in R using the qpcR package version 1.4 (ref. 47). A seven-parameter sigmoidal model was fit on each PCR curve. The same model was also used for background subtraction. The second derivative maximum of the fit was defined as the C_p value. The efficiency of a PCR reaction was estimated as the mean of all sigmoidal efficiencies in its replicates. Expression levels were averaged over technical and biological replicates, and normalized to the expression level of the *mrlp-40* gene via permutation approach.

Generation of *daf-9;*ΔΔ*tps*. *tps-1* males were crossed to *daf-9(dh6);dhEx24* and then GFP-positive hermaphrodites from the first generation were crossed to *tps-1* males. Self-fertilization of second-generation GFP-positive hermaphrodites gave third generation of GFP-positive hermaphrodites and these worms were singled to give *daf-9(dh6),tps-1(ok373);dhEx24*. The strains were selected for being GFP-positive, homozygous for *tps-1* (tested using PCR), and producing dauer-like larvae. *daf-9(dh6),tps-1(ok373);dhEx24* hermaphrodites were then crossed to *tps-2* males, and GFP-positive males from the progeny were backcrossed to *daf-9(dh6),tps-1(ok373);dhEx24*. Second-generation GFP-positive hermaphrodites were self-fertilized to give fraction of *tps-2(ok526);daf-9(dh6),tps-1(ok373);dhEx24* worms in the third generation. Strains were again controlled for GFP signal; PCR for verification of the homozygous state of *tps-2* and *tps-1* was carried out and the Daf-c phenotype was inspected. Generally, none of the *tps-2(ok526);daf-9(dh6), tps-1(ok373);dhEx24* strains were able to produce GFP-negative L4 larvae or adult worms. For the production of such worms, (25S)-Δ^7 DA was added to the feeding media, which resulted in the formation of fertile adult *daf-9(dh6);*ΔΔ*tps*.

Generation of *daf-2(e1368);*ΔΔ*tps*. *daf-2(e1368)* males were crossed to *tps-2(ok526);tps-1(ok373)* hermaphrodites and the resulting males were backcrossed to *tps-2(ok526);tps-1(ok373)*. The second-generation hermaphrodites were separated to self-fertilize. Third-generation larvae were grown on non-permissive temperature (25 °C) and individuals, which developed into dauer larvae, were selected. These were shifted to permissive temperature (15 °C) so that they could exit from the dauer state and self-fertilize to give fraction of triple-homozygous *tps-2(ok526);daf-2(e1368);tps-1(ok373)* mutants. Strains were quality-controlled using PCR and dauer phenotypic assays.

Generation of *daf-7;idh-1*. Males heterozygous for *idh-1(ok2832)* were crossed to *daf-7(e1372)* hermaphrodites. The hermaphrodites from the progeny laid eggs that at 25 °C developed into dauers or adults. The dauers were relocated to 15 °C to re-enter reproduction and their progeny was screened using PCR for homozygous *daf-7(e1372);idh-1(ok2832)* individuals.

Overexpression of *tps-1*::eGFP in *daf-7*. The *tps-1*-containing fosmid WRM0628cF08 was recombineered by C-terminal tagging of the *tps-1* gene (ZK54.2) with eGFP optimized for *C. elegans*. This was performed via a procedure modified from literature[48] where improved plasmids pRedFlp4 and pPUBH were used instead of the original pRedFlp and pPUB. However, WRM0628cF08 contained several additional genes. To eliminate them, the construct was engineered so that only eGFP-tagged *tps-1*-coding sequence with its corresponding 5′- and 3′-untranslated repeats and ~5 kB promoter region remained in it (Fig. 2a). For that, a subcloning cassette was prepared using PCR amplification from the pPUBH plasmid using a specific pair of primers. The sequences of the primers can be seen in Supplementary Table 3. The first 50 bp (homology arms) are specific to the *tps-1* sequence; the rest of the sequence is specific to pPUBH plasmid sequence. The host cells containing the original fosmid construct were transformed with the subcloning cassette via electroporation. Transformants were selected by blasticidin resistance and the presence of the new construct was confirmed via fingerprinting by XbaI digestion.

The new construct was then bombarded into *unc-119* worms and eGFP-positive worms without unc phenotype were selected. The progeny of these transgenes was followed for several generations and, according to the segregation of the eGFP signal, it was confirmed that the construct existed as an extrachromosomal array.

To introduce the *tps-1*::eGFP in *daf-7(e1372)* background, *tps-1*::eGFP was first outcrossed twice to N2 and then eGFP-positive males were crossed to *daf-7* hermaphrodites. eGFP-positive hermaphrodites of the progeny were let to lay eggs at 25 °C to form eGFP-positive dauer larvae, which would be candidates for homozygous *daf-7* with *tps-1*::eGFP. eGFP-positive dauer larvae were singled in 12-well NGM plates with NA22 bacteria and supplemented with 1.3 µM (25S)-Δ^7 DA to resume reproductive development. Strains were examined for several generations for dauer formation and strong eGFP signal.

References

1. Riddle, D. L. & Albert, P. S. in *C.elegans II*. (eds Riddle, D. L., Blumenthal, T., Meyer, J. B. & Priess, J. R.) 739–768 (Cold Spring Harbor Laboratory Press, 1997).
2. Cassada, R. C. & Russell, R. L. The dauerlarva, a post-embryonic developmental variant of the nematode *Caenorhabditis elegans*. *Dev. Biol.* **46,** 326–342 (1975).
3. Erkut, C. *et al.* Trehalose renders the dauer larva of *Caenorhabditis elegans* resistant to extreme desiccation. *Curr. Biol.* **21,** 1331–1336 (2011).
4. McElwee, J. J., Schuster, E., Blanc, E., Thornton, J. & Gems, D. Diapause-associated metabolic traits reiterated in long-lived daf-2 mutants in the nematode *Caenorhabditis elegans*. *Mech. Ageing Dev.* **127,** 458–472 (2006).
5. Erkut, C. *et al.* Molecular strategies of the *Caenorhabditis elegans* dauer larva to survive extreme desiccation. *PLoS ONE* **8,** e82473 (2013).
6. Golden, T. R. & Melov, S. Gene expression changes associated with aging in *C. elegans*. *WormBook* **12,** 1–12 (2007).
7. Erkut, C. & Kurzchalia, T. V. The *C. elegans* dauer larva as a paradigm to study metabolic suppression and desiccation tolerance. *Planta* **242,** 389–396 (2015).
8. Jeong, P. Y. *et al.* Chemical structure and biological activity of the *Caenorhabditis elegans* dauer-inducing pheromone. *Nature* **433,** 541–545 (2005).
9. Butcher, R. A., Fujita, M., Schroeder, F. C. & Clardy, J. Small-molecule pheromones that control dauer development in *Caenorhabditis elegans*. *Nat. Chem. Biol.* **3,** 420–422 (2007).
10. Antebi, A., Culotti, J. G. & Hedgecock, E. M. daf-12 regulates developmental age and the dauer alternative in *Caenorhabditis elegans*. *Development* **125,** 1191–1205 (1998).
11. Antebi, A., Yeh, W. H., Tait, D., Hedgecock, E. M. & Riddle, D. L. daf-12 encodes a nuclear receptor that regulates the dauer diapause and developmental age in *C. elegans*. *Genes Dev.* **14,** 1512–1527 (2000).
12. Mahanti, P. *et al.* Comparative metabolomics reveals endogenous ligands of DAF-12, a nuclear hormone receptor, regulating *C. elegans* development and lifespan. *Cell Metab.* **19,** 73–83 (2014).
13. Motola, D. L. *et al.* Identification of ligands for DAF-12 that govern dauer formation and reproduction in *C. elegans*. *Cell* **124,** 1209–1223 (2006).
14. Gerisch, B., Weitzel, C., Kober-Eisermann, C., Rottiers, V. & Antebi, A. A hormonal signaling pathway influencing *C. elegans* metabolism, reproductive development, and life span. *Dev. Cell* **1,** 841–851 (2001).
15. Hannich, J. T. *et al.* Methylation of the sterol nucleus by STRM-1 regulates dauer larva formation in *Caenorhabditis elegans*. *Dev. Cell* **16,** 833–843 (2009).
16. Penkov, S. *et al.* Maradolipids: diacyltrehalose glycolipids specific to dauer larva in *Caenorhabditis elegans*. *Angew. Chem. Int. Ed. Engl.* **49,** 9430–9435 (2010).
17. Pellerone, F. I. *et al.* Trehalose metabolism genes in *Caenorhabditis elegans* and filarial nematodes. *Int. J. Parasitol.* **33,** 1195–1206 (2003).
18. Kormish, J. D. & McGhee, J. D. The *C. elegans* lethal gut-obstructed gob-1 gene is trehalose-6-phosphate phosphatase. *Dev. Biol.* **287,** 35–47 (2005).
19. Ren, P. *et al.* Control of *C. elegans* larval development by neuronal expression of a TGF-beta homolog. *Science* **274,** 1389–1391 (1996).
20. Schackwitz, W. S., Inoue, T. & Thomas, J. H. Chemosensory neurons function in parallel to mediate a pheromone response in *C. elegans*. *Neuron* **17,** 719–728 (1996).
21. Swanson, M. M. & Riddle, D. L. Critical periods in the development of the *Caenorhabditis elegans* dauer larva. *Dev. Biol.* **84,** 27–40 (1981).
22. Gerisch, B. & Antebi, A. Hormonal signals produced by DAF-9/cytochrome P450 regulate *C. elegans* dauer diapause in response to environmental cues. *Development* **131,** 1765–1776 (2004).
23. Gottlieb, S. & Ruvkun, G. daf-2, daf-16 and daf-23: genetically interacting genes controlling Dauer formation in *Caenorhabditis elegans*. *Genetics* **137,** 107–120 (1994).

24. Gems, D. *et al.* Two pleiotropic classes of daf-2 mutation affect larval arrest, adult behavior, reproduction and longevity in *Caenorhabditis elegans*. *Genetics* **150,** 129–155 (1998).
25. Matyash, V. *et al.* Sterol-derived hormone(s) controls entry into diapause in *Caenorhabditis elegans* by consecutive activation of DAF-12 and DAF-16. *PLoS Biol.* **2,** e280 (2004).
26. Held, J. M. *et al.* DAF-12-dependent rescue of dauer formation in *Caenorhabditis elegans* by (25S)-cholestenoic acid. *Aging Cell* **5,** 283–291 (2006).
27. Sarov, M. *et al.* A genome-scale resource for in vivo tag-based protein function exploration in *C. elegans*. *Cell* **150,** 855–866 (2012).
28. Wamelink, M. M., Struys, E. A. & Jakobs, C. The biochemistry, metabolism and inherited defects of the pentose phosphate pathway: a review. *J. Inherit. Metab. Dis.* **31,** 703–717 (2008).
29. Waskell, L. & Kim, J.-J. P. in *Cytochrome P450* 33–68 (Springer International Publishing, 2015).
30. Kamath, R. S. *et al.* Systematic functional analysis of the *Caenorhabditis elegans* genome using RNAi. *Nature* **421,** 231–237 (2003).
31. Frezza, C., Tennant, D. A. & Gottlieb, E. IDH1 mutations in gliomas: when an enzyme loses its grip. *Cancer Cell* **17,** 7–9 (2010).
32. Lamitina, S. T. & Strange, K. Transcriptional targets of DAF-16 insulin signaling pathway protect *C. elegans* from extreme hypertonic stress. *Am. J. Physiol. Cell Physiol.* **288,** C467–C474 (2005).
33. Murphy, C. T. *et al.* Genes that act downstream of DAF-16 to influence the lifespan of *Caenorhabditis elegans*. *Nature* **424,** 277–283 (2003).
34. Fielenbach, N. & Antebi, A. *C. elegans* dauer formation and the molecular basis of plasticity. *Genes Dev.* **22,** 2149–2165 (2008).
35. Albert, P. S. & Riddle, D. L. Mutants of *Caenorhabditis elegans* that form dauer-like larvae. *Dev. Biol.* **126,** 270–293 (1988).
36. Jia, K., Albert, P. S. & Riddle, D. L. DAF-9, a cytochrome P450 regulating *C. elegans* larval development and adult longevity. *Development* **129,** 221–231 (2002).
37. Mak, H. Y. & Ruvkun, G. Intercellular signalling of reproductive development by the *C. elegans* DAF-9 cytochrome p450. *Development* **131,** 1777–1786 (2004).
38. Schaedel, O. N., Gerisch, B., Antebi, A. & Sternberg, P. W. Hormonal signal amplification mediates environmental conditions during development and controls an irreversible commitment to adulthood. *PLoS Biol.* **10,** e1001306 (2012).
39. Burnell, A. M., Houthoofd, K., O'Hanlon, K. & Vanfleteren, J. R. Alternate metabolism during the dauer stage of the nematode *Caenorhabditis elegans*. *Exp. Gerontol.* **40,** 850–856 (2005).
40. Martin, R., Dabritz, F., Entchev, E. V., Kurzchalia, T. V. & Knolker, H. J. Stereoselective synthesis of the hormonally active (25S)-delta7-dafachronic acid, (25S)-Delta4-dafachronic acid, (25S)-dafachronic acid, and (25S)-cholestenoic acid. *Org. Biomol. Chem.* **6,** 4293–4295 (2008).
41. Martin, R. *et al.* Improved synthesis of an ascaroside pheromone controlling dauer larva development in *Caenorhabditis elegans*. *Synthesis (Mass)* **2009,** 3488–3492 (2009).
42. Saini, R. *et al.* Stereoselective synthesis and hormonal activity of novel dafachronic acids and naturally occurring steroids isolated from corals. *Org. Biomol. Chem.* **10,** 4159–4163 (2012).
43. Brenner, S. The genetics of *Caenorhabditis elegans*. *Genetics* **77,** 71–94 (1974).
44. Ferrari, S. L. P. & Cribari-Neto, F. Beta regression for modelling rates and proportions. *J. Appl. Stat.* **31,** 799–815 (2004).
45. Bligh, E. G. & Dyer, W. J. A rapid method of total lipid extraction and purification. *Can. J. Biochem. Physiol.* **37,** 911–917 (1957).
46. Randerath, E. & Randerath, K. Resolution of complex nucleotide mixtures by two-dimensional anion-exchange thin-layer chromatography. *J. Chromatogr.* **16,** 126–129 (1964).
47. Ritz, C. & Spiess, A. N. qpcR: an R package for sigmoidal model selection in quantitative real-time polymerase chain reaction analysis. *Bioinformatics* **24,** 1549–1551 (2008).
48. Sarov, M. *et al.* A recombineering pipeline for functional genomics applied to *Caenorhabditis elegans*. *Nat. Methods* **3,** 839–844 (2006).

Acknowledgements

We thank all members of the Kurzchalia laboratory for helpful discussions, and Diego de Mendoza and Eugeni Entchev for critical reading of the manuscript. We are grateful to CGC and to Adam Antebi for providing worm strains and to Hans-Joachim Knölker for the synthesis of various organic compounds.

Author contributions

S.P. and T.V.K. designed research; S.P., D.K., C.E. and F.M. performed research; M.S. and C.E. contributed to generation of transgenic *C. elegans* strains; S.P., C.E. and T.V.K. analysed data; all authors discussed the data; and S.P., C.E. and T.V.K. wrote the paper.

Additional information

Supplementary Information accompanies this paper at http://www.nature.com/naturecommunications

Competing financial interests: The authors declare no competing financial interests.

Reprints and permission information is available online at http://npg.nature.com/reprintsandpermissions/

How to cite this article: Penkov, S. *et al.* Integration of carbohydrate metabolism and redox state controls dauer larva formation in *Caenorhabditis elegans*. *Nat. Commun.* 6:8060 doi: 10.1038/ncomms9060 (2015).